Science Advances
AAAS

advances.sciencemag.org/cgi/content/full/5/8/eaaw8330/DC1

Supplementary Materials for

Aging promotes reorganization of the CD4 T cell landscape toward extreme regulatory and effector phenotypes

Yehezqel Elyahu, Idan Hekselman, Inbal Eizenberg-Magar, Omer Berner, Itai Strominger, Maya Schiller, Kritika Mittal, Anna Nemirovsky, Ekaterina Eremenko, Assaf Vital, Eyal Simonovsky, Vered Chalifa-Caspi, Nir Friedman, Esti Yeger-Lotem*, Alon Monsonego*

*Corresponding author. Email: alonmon@bgu.ac.il (A.M.); estiyl@bgu.ac.il (E.Y.-L.)

Published 21 August 2019, *Sci. Adv.* **5**, eaaw8330 (2019)
DOI: 10.1126/sciadv.aaw8330

The PDF file includes:

Other Supplementary Material for this manuscript includes the following:

(available at advances.sciencemag.org/cgi/content/full/5/8/eaaw8330/DC1)

A

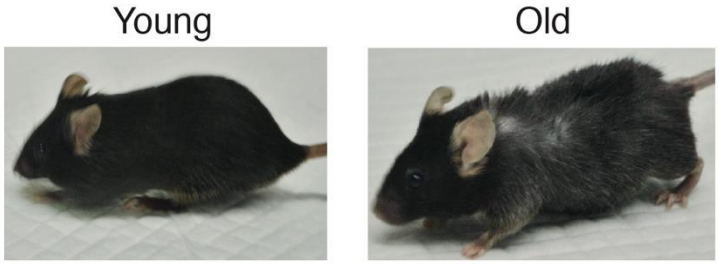

B

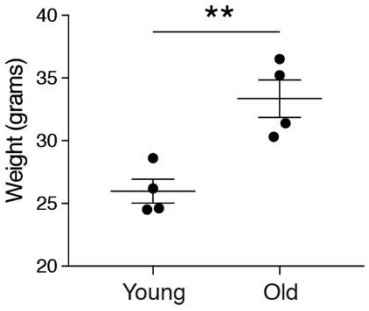

C

Gating strategy:

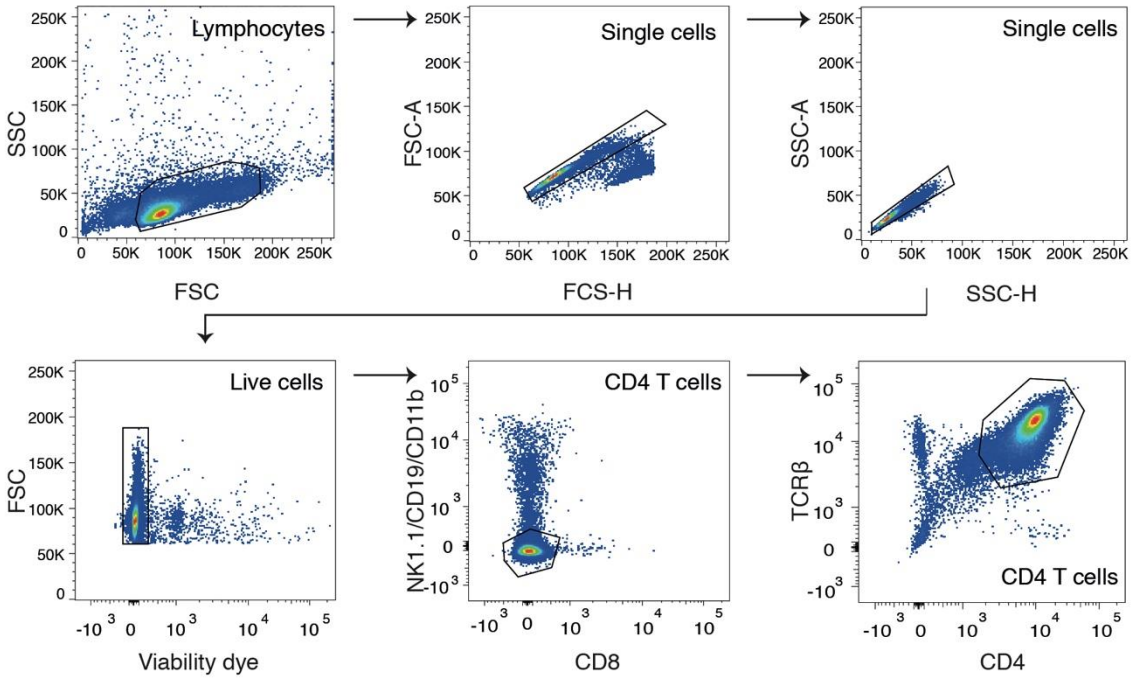

D

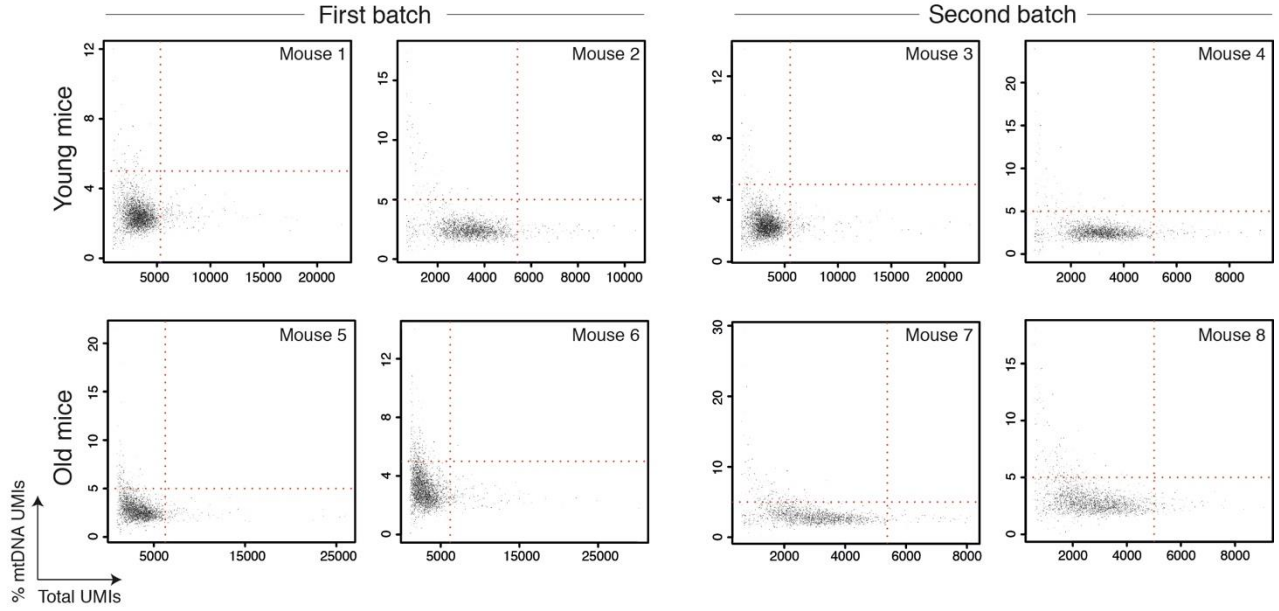

Fig. S1. Purification of CD4 T cells from young and old mice. (A) Representative pictures of young (2 month) and old (24 month) mice used for the single-cell RNA-sequencing (scRNA-seq) experiments. Mice were examined for macroscopic abnormalities. In the old group, except for visible hair loss, no wounds or other skin abnormalities were observed. **(B)** Weight differences between young and old mice used for the scRNA-seq experiments. As expected, old mice had higher weights than young mice (https://www.jax.org/jax-mice-and-services/strain-data-sheet-pages/body-weight-chart-aged-b6). Each dot represents an individual mouse, and the horizontal lines indicate the mean ±SEM ($p=0.0059$). **(C)** Gating strategy for sorting highly pure CD4 T cells used for the scRNA-seq experiments. Enriched CD4 T cells were sorted as $CD4^{+}TCRb^{+}live\text{-}cells^{+}doublets^{-}CD8^{-}NK1.1^{-}CD19^{-}CD11b^{-}$. **(D)** Quality control (QC) of cells for further scRNAseq analyses. X axis shows the total number of unique molecular identifiers (UMIs) of cells in each mouse. To discard doublets, cells were ordered by their UMIs, and the top (N/1,000) % of cells per sample were filtered out, where *N* is the number of cells identified for each mouse; threshold marked with red, dashed vertical line. Y axis shows the percentage of mitochondrial DNA-associated (mtDNA) UMIs out of total number of UMIs of cells in each mouse. To disregard lysed cells with retained mitochondrial RNA, cells with more than 5% UMIs mapped to mitochondrial DNA were filtered out; threshold marked with red, dashed horizontal line. **$p<0.01$ (unpaired T test). (Photo credit: Yehezqel Elyahu, Ben Gurion University of the Negev, Beer-Sheva, Israel).

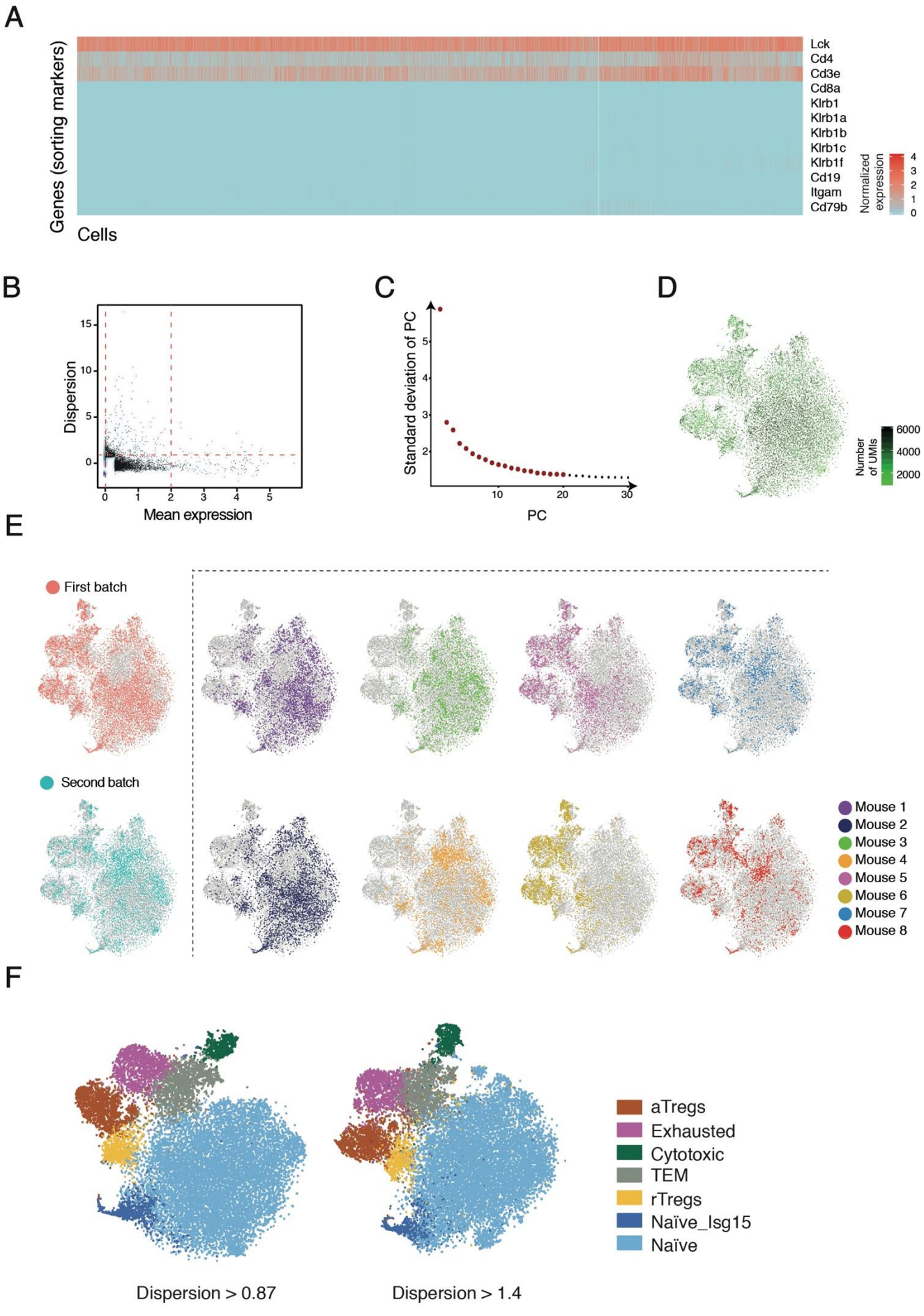
A
Genes (sorting markers)
Cells
Lck
Cd4
Cd3e
Cd8a
Klrb1
Klrb1a
Klrb1b
Klrb1c
Klrb1f
Cd19
Itgam
Cd79b
Normalized expression
4
3
2
1
0
B
Dispersion
Mean expression
C
Standard deviation of PC
PC
D
Number of UMIs
6000
4000
2000
E
First batch
Second batch
Mouse 1
Mouse 2
Mouse 3
Mouse 4
Mouse 5
Mouse 6
Mouse 7
Mouse 8
F
aTregs
Exhausted
Cytotoxic
TEM
rTregs
Naïve_Isg15
Naïve
Dispersion > 0.87
Dispersion > 1.4

Fig. S2. Dimensionality reduction of scRNA-seq data. (A) A heatmap showing normalized expression of genes indicating highly pure CD4 T cells. Gene expression patterns indicate a highly pure population of CD4 T cells. **(B)** The relationship between gene expression and dispersion. Each dot represents a gene; the X and Y axes represent its mean expression and dispersion (defined as log(variance/mean)), respectively. Dashed lines show the thresholds used for the definition of variable genes (mean expression between 0.0125 and 2 and dispersion above 0.9). **(C)** The standard deviation of top 30 principal components (PCs) was calculated using the expression of variable genes. The first 20 PCs were used for further dimensionality reduction and clustering (marked in red). **(D-E)** T-SNE projections of CD4 T cells, colored by number of UMIs within all cells (D) and by mouse of origin (E) (mice names correspond to fig. S1D). **(F)** T-SNEs projections of all CD4 T cells, where dimensionality reduction process was based on variable genes selected with minimal dispersion thresholds of 0.87 (left) and 1.4 (right). Cell subsets were colored according to Fig. 2A.

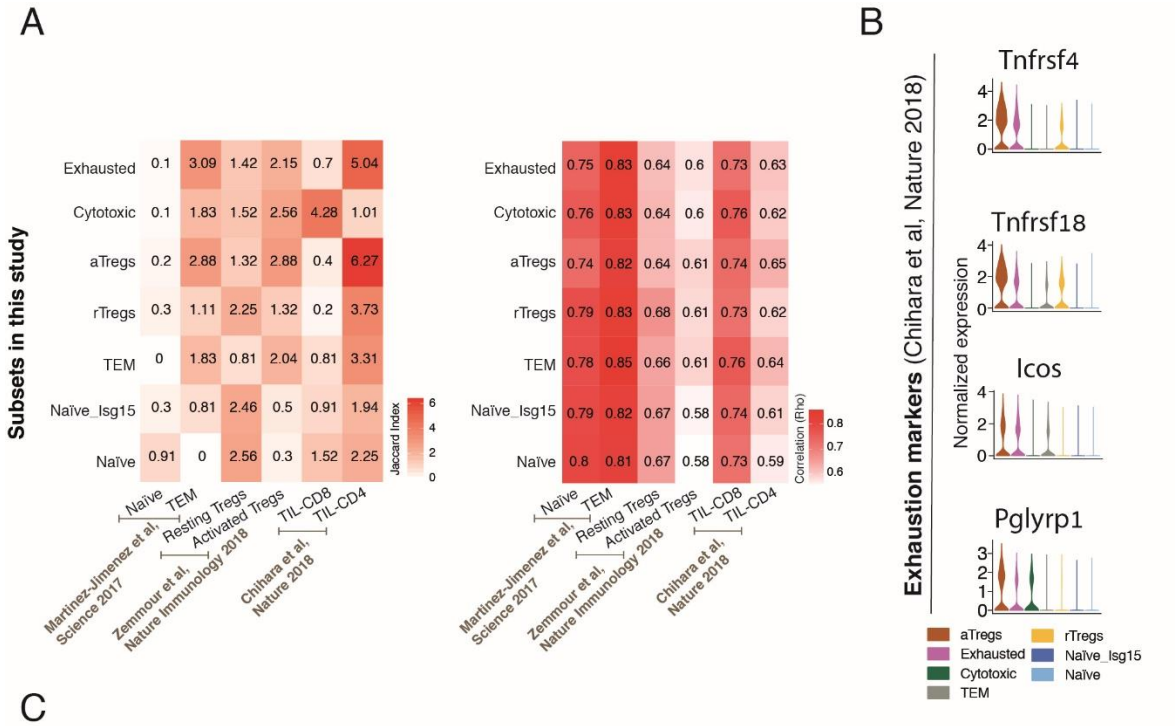

C

Young mice

Mouse 1

n = 4,097

2.3% aTregs
1.2% Exhausted
0.5% Cytotoxic
4.5% TEM
4.7% rTregs
4.1% Naïve_Isg15
82.6% Naïve

Mouse 2

n = 3,927

2.2% aTregs
1.2% Exhausted
0.4% Cytotoxic
4.9% TEM
3.4% rTregs
6.6% Naïve_Isg15
81.3% Naïve

Mouse 3

n = 2,614

0.9% aTregs
0.4% Exhausted
0.1% Cytotoxic
4.8% TEM
3.1% rTregs
4.7% Naïve_Isg15
86.0% Naïve

Mouse 4

n = 2,548

0.9% aTregs
0.2% Exhausted
0.1% Cytotoxic
3.1% TEM
4.8% rTregs
6.3% Naïve_Isg15
84.4% Naïve

Old mice

Mouse 5

n = 3,068

15.7% aTregs
14.5% Exhausted
4.5% Cytotoxic
15.6%TEM
3.6% aTregs
3.5% Naïve_Isg15
42.6% Naïve

Mouse 6

n = 3,332

24.3% aTregs
22.0% Exhausted
10.8% Cytotoxic
15.5% TEM
4.4% aTregs
3.9% Naïve_Isg15
19.1% Naïve

Mouse 7

n = 2,044

9.0% aTregs
10.2% Exhausted
3.2% Cytotoxic
12.2% TEM
5.3% aTregs
2.4% Naïve_Isg15
57.6% Naïve

Mouse 8

n = 2,377

9.0% aTregs
12.7% Exhausted
9.0% Cytotoxic
14.9% TEM
3.2% aTregs
3.2% Naïve_Isg15
48.0% Naïve

Fig. S3. Subset identity and abundance in mice used for scRNA-seq. (A) Heatmaps presenting CD4 T-cell subset similarities between this study and previously published datasets: a dataset of naïve and TEM subsets *(16)*; a dataset of Tregs in resting and activated states *(21)*, pertinent to our Tregs subsets; and a dataset of tumor-infiltrating lymphocytes (TIL; *(22)*), related to our cytotoxic and exhausted subsets. Left: Jaccard index-based metric comparing gene signatures of each pair of subsets, implemented via the matchSCore package (*(62)*; distances were multiplied by 100). Gene signatures were defined as the top 500 most up-regulated genes of each subset, relative to other subsets taken from the same study (a pseudocount of 1 was added to the expression level of each gene, to allow fold-change analysis). Right: Spearman correlation coefficients between the gene expression profiles of each pair of subsets. Expression profiles included only genes expressed above noise levels (mean normalized expression > 0.0125) in both subsets, resulting in at least 7,400 genes per comparison. **(B)** Violin plots showing key marker genes of exhaustion highly expressed in the exhausted and aTregs subsets. Markers were chosen based on Chihara et al, Nature 2018 *(22)* that showed a common co-inhibitory gene module, shared by exhausted CD4 and CD8 T lymphocytes. **(C)** Pie charts showing the proportion of the different cell subsets per mouse. The number of cells per mouse (n) is noted below each pie chart. Colors correspond to subset identity. Above: Young mice, Below: Old mice.

A

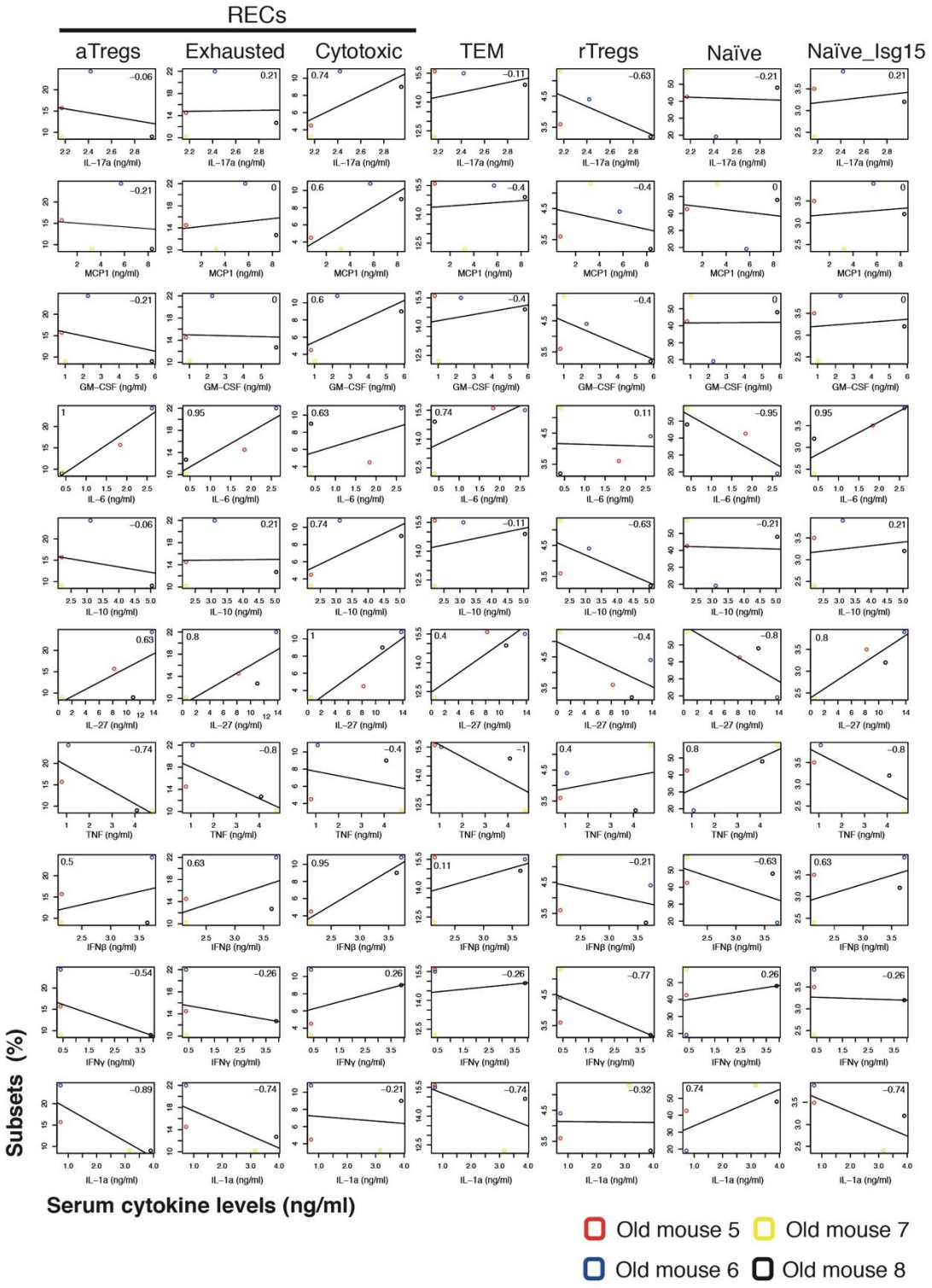
RECs
aTregs
Exhausted
Cytotoxic
TEM
rTregs
Naïve
Naïve_Isg15
IL−17a (ng/ml)
MCP1 (ng/ml)
GM−CSF (ng/ml)
IL−6 (ng/ml)
IL−10 (ng/ml)
IL−27 (ng/ml)
TNF (ng/ml)
IFNβ (ng/ml)
IFNγ (ng/ml)
IL−1a (ng/ml)
Subsets (%)
Serum cytokine levels (ng/ml)
Old mouse 5
Old mouse 7
Old mouse 6
Old mouse 8

B

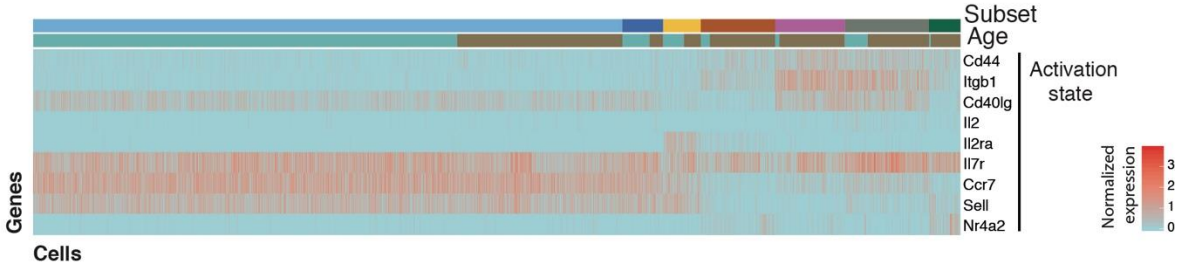
Subset
Age
Cd44
Itgb1
Cd40lg
Il2
Il2ra
Il7r
Ccr7
Sell
Nr4a2
Activation state
Genes
Cells
Normalized expression
3
2
1
0

Fig. S4. RECs activation state and correlation with serum cytokines. (A) Scatter plots showing Spearman correlation coefficients between the levels of cytokines measured in serum (ng/ml), and the frequency of each subset (%) within the spleen of mice used for scRNA-seq experiments, in X- and Y-axis, respectively. Each dot represents a mouse, and the number in the top corner represents the correlation coefficient. **(B)** A heatmap showing normalized expression of genes associated with the activation state of CD4 T cells. All CD4 T cells were grouped by subset and age (horizontal bars), as in Fig. 2B. The cytotoxic, exhausted and TEM subsets showed a higher activation state.

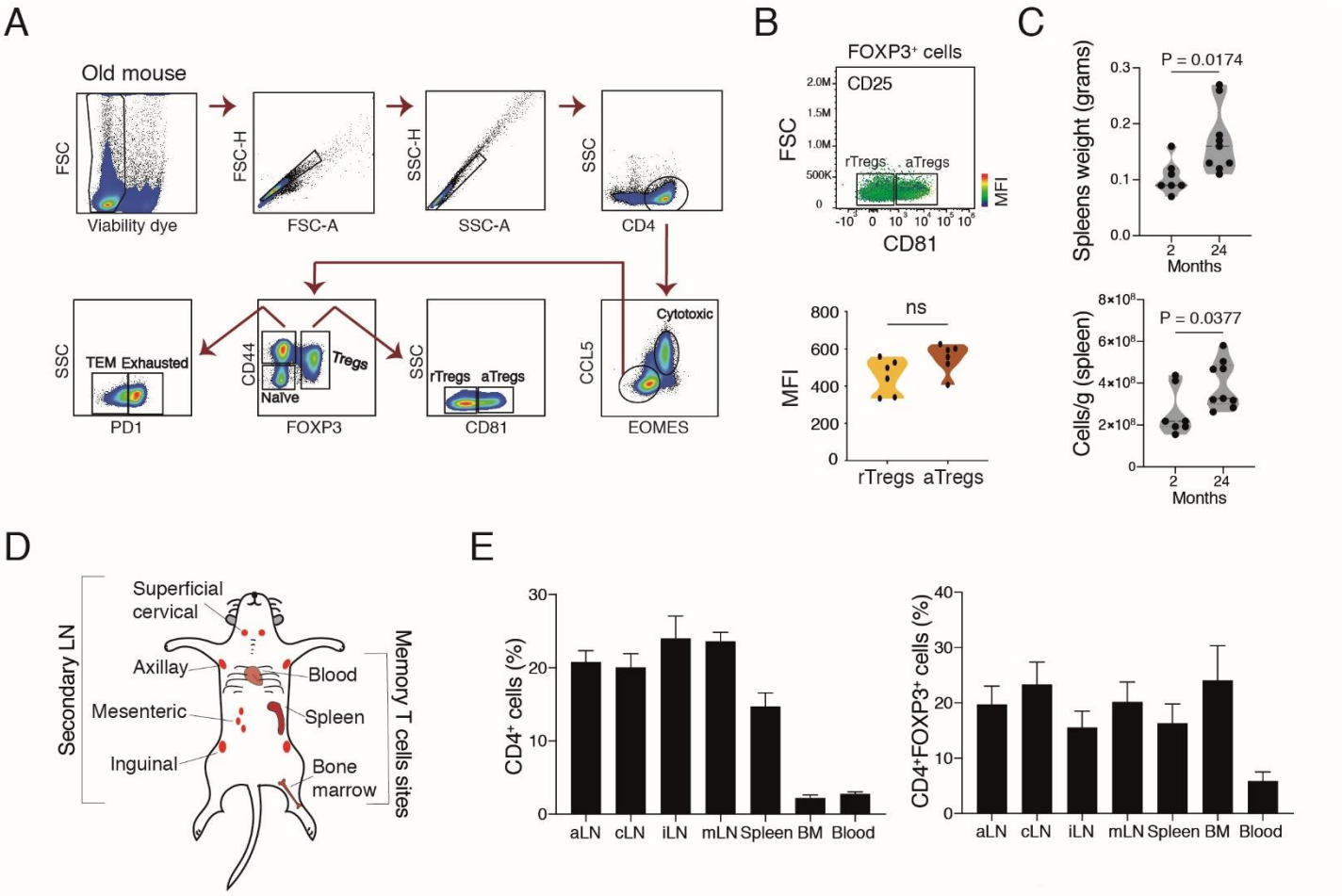

p-values:

	aLN	cLN	iLN	mLN	Spleen	BM	Blood
aLN		ns	ns	ns	0.0035	0.0011	0.0089
cLN			ns	ns	0.0068	0.0044	0.154
iLN				0.0105	0.0017	0.0015	0.0122
mLN					0.007	0.0055	0.0178
Spleen						ns	0.0474
BM							ns
Blood							

p-values:

	aLN	cLN	iLN	mLN	Spleen	BM	Blood
aLN		ns	ns	ns	ns	0.0017	ns
cLN			ns	ns	ns	0.0001	ns
iLN				ns	ns	0.0003	ns
mLN					ns	0.0001	ns
Spleen						0.0111	ns
BM							0.0096
Blood							

p-values:

	aLN	cLN	iLN	mLN	Spleen	BM	Blood
aLN		0.0018	ns	ns	0.0073	0.0002	0.0014
cLN			ns	ns	ns	0.0004	0.039
iLN				ns	0.0273	0.0002	0.0024
mLN					ns	0.0001	0.0296
Spleen						ns	0.0474
BM							0.0167
Blood							

Fig. S5. RECs abundance with time and across different immunological sites. (A) Representative flow cytometry plots from old mouse (24 months) showing the gating strategy used to differentiate between old CD4 T-cell subsets. Cytotoxic, naïve, exhausted, TEM, rTregs and aTregs subsets are shown. **(B)** Representative flow cytometry plots gated on $FOXP3^+$ cells showing the MFI of CD25, projected on $CD81^-$ (rTregs) and $CD81^+$ (aTregs) populations (top panel). A graph showing CD25 MFI values in rTregs and aTregs (bottom panel). No significant difference was observed. Each dot represents one mouse (n=6, from two different experiments). **(C)** Graphs showing the weight of spleens (grams, top plot) and the number of cells per gram spleen (bottom plot) in young (n=7, 2 months) and old (n=9, 24 months) mice. Spleens from old mice had a significantly higher weight and cell number per g/spleen, than spleens from young mice (data from one representative experiment, Student t-test). **(D)** Illustration of immune compartments collected for experiments (Fig. 4, D to F). **(E)** The percentage of CD4 T cells out of total cells (after discarding dead cells and doublets) (left) and the percentage of $FOXP3^+$ cells out of $CD4^+$ cells (right), across different immune sites. **(F)** Bar plots and tables showing the significance of differences of each REC in different immune sites. Data were collected from three different experiments (n=2-3 mice for each experiment). One-way ANOVA test with Tukey correction for multiple comparisons. aLN, cLN, iLN and mLN = axillary, cervical, inguinal and mesenteric lymph nodes, respectively. BM = bone marrow. Bars colored similarly correspond to the same mouse.

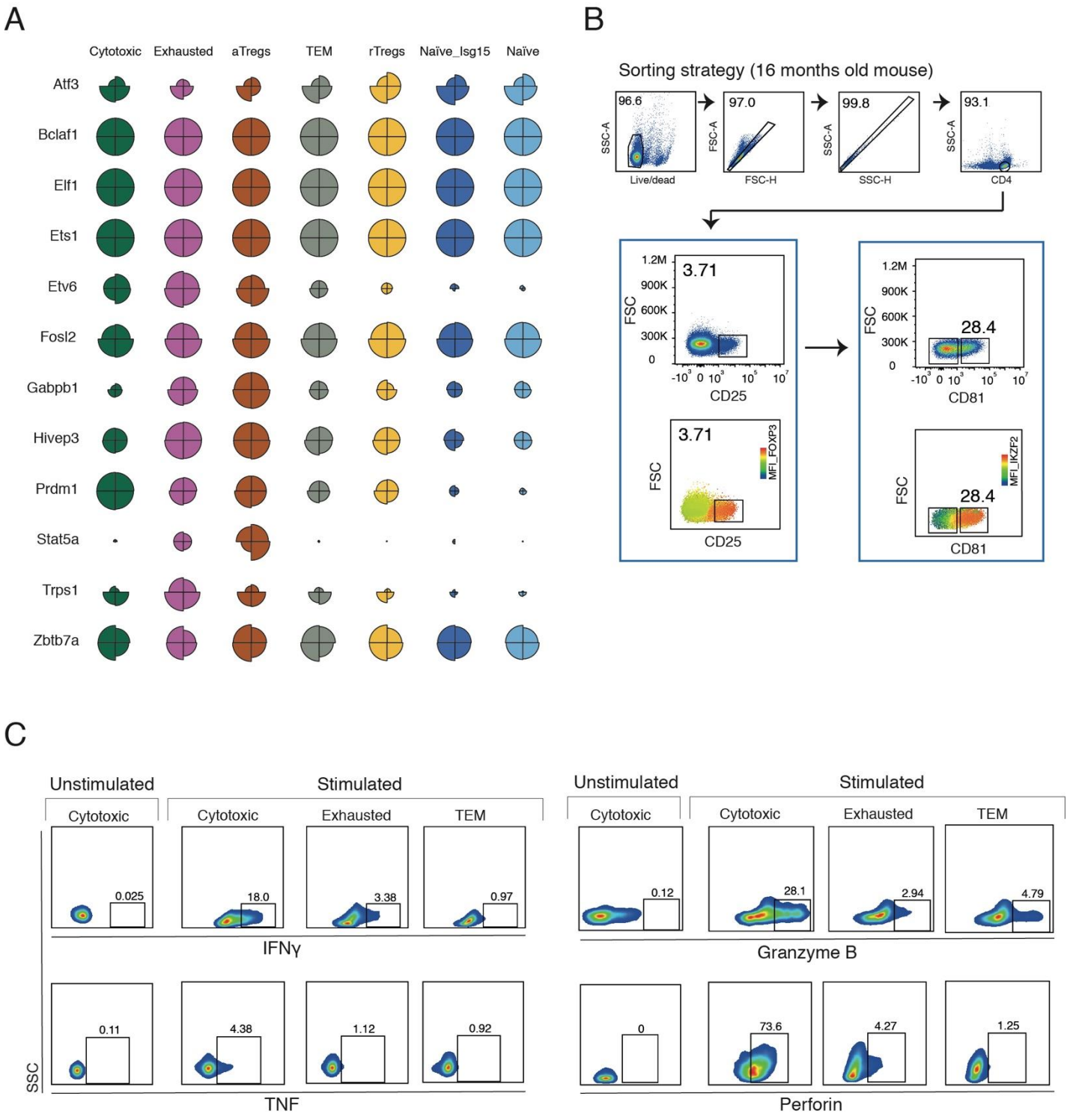
A
Cytotoxic
Exhausted
aTregs
TEM
rTregs
Naïve_Isg15
Naïve
Atf3
Bclaf1
Elf1
Ets1
Etv6
Fosl2
Gabpb1
Hivep3
Prdm1
Stat5a
Trps1
Zbtb7a
B
Sorting strategy (16 months old mouse)
96.6
SSC-A
Live/dead
97.0
FSC-A
FSC-H
99.8
SSC-A
SSC-H
93.1
SSC-A
CD4
1.2M
900K
600K
300K
0
FSC
3.71
CD25
3.71
MFI_FOXP3
FSC
CD25
1.2M
900K
600K
300K
0
FSC
28.4
CD81
28.4
MFI_IKZF2
FSC
CD81
C
Unstimulated
Stimulated
Cytotoxic
Cytotoxic
Exhausted
TEM
0.025
18.0
3.38
0.97
IFNγ
0.11
4.38
1.12
0.92
SSC
TNF
Unstimulated
Stimulated
Cytotoxic
Cytotoxic
Exhausted
TEM
0.12
28.1
2.94
4.79
Granzyme B
0
73.6
4.27
1.25
Perforin

Fig. S6. Gene regulatory networks and cytokine secretion in RECs. (A) Radared-balloon plot showing the magnitude of activity of selected regulons across subsets. Slices of the balloons represent the percentage of cells with activated regulons in each mouse. All slices of the same regulon are normalized to the maximal slice of that regulon across mice and subsets. Colors correspond to subsets (Fig. 2A). (B) Sorting strategy used to isolate rTregs ($CD25^{high}CD81^{-}$) and aTregs ($CD25^{high}CD81^{+}$) out of $CD4^{+}$ cells. To validate Tregs identity, the MFIs of FOXP3 and IKZF2 were measured in $CD4^{+}$ and $CD4^{+}CD25^{+}$ cells, respectively, before sorting. (C) Representative flow cytometry plots showing unstimulated versus stimulated cells in the cytotoxic, exhausted and TEM subsets analyzed for expression of IFNγ, TNF, granzyme B and perforin proteins.

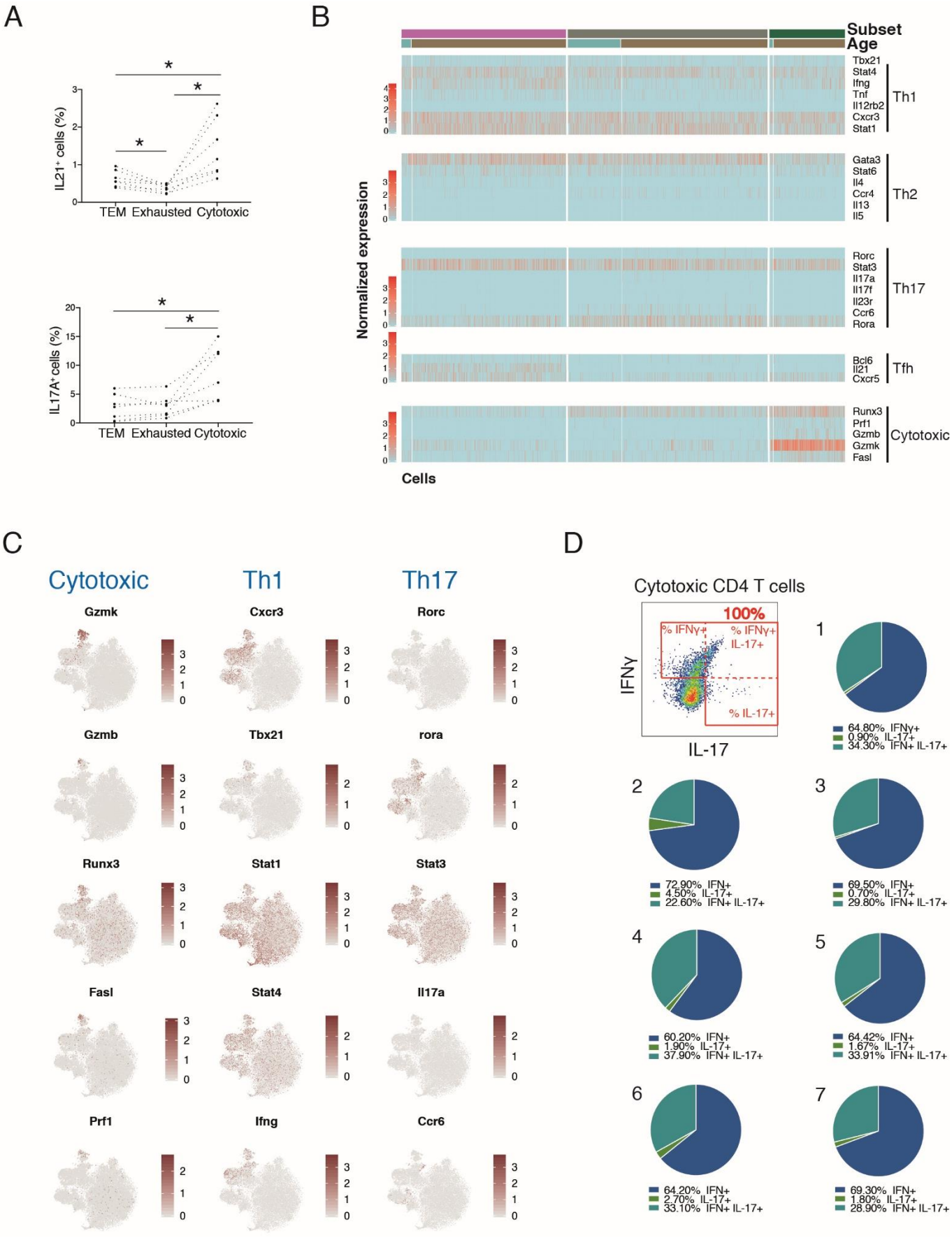
A
IL21+ cells (%)
TEM Exhausted Cytotoxic
IL17A+ cells (%)
TEM Exhausted Cytotoxic
B
Subset
Age
Normalized expression
Tbx21
Stat4
Ifng
Tnf
Il12rb2
Cxcr3
Stat1
Th1
Gata3
Stat6
Il4
Ccr4
Il13
Il5
Th2
Rorc
Stat3
Il17a
Il17f
Il23r
Ccr6
Rora
Th17
Bcl6
Il21
Cxcr5
Tfh
Runx3
Prf1
Gzmb
Gzmk
Fasl
Cytotoxic
Cells
C
Cytotoxic
Th1
Th17
Gzmk
Cxcr3
Rorc
Gzmb
Tbx21
rora
Runx3
Stat1
Stat3
Fasl
Stat4
Il17a
Prf1
Ifng
Ccr6
D
Cytotoxic CD4 T cells
100%
% IFNγ+
% IFNγ+ IL-17+
% IL-17+
IFNγ
IL-17
1
64.80% IFNγ+
0.90% IL-17+
34.30% IFN+ IL-17+
2
72.90% IFN+
4.50% IL-17+
22.60% IFN+ IL-17+
3
69.50% IFN+
0.70% IL-17+
29.80% IFN+ IL-17+
4
60.20% IFN+
1.90% IL-17+
37.90% IFN+ IL-17+
5
64.42% IFN+
1.67% IL-17+
33.91% IFN+ IL-17+
6
64.20% IFN+
2.70% IL-17+
33.10% IFN+ IL-17+
7
69.30% IFN+
1.80% IL-17+
28.90% IFN+ IL-17+

Fig. S7. Characterization of T helper polarizations within RECs. (A) Validation of Rora TF program activation in TEM, exhausted and cytotoxic cells. The percentage of $IL21^+$ (upper panel) and $IL17a^+$ (lower panel) cells were significantly higher within the cytotoxic cells. Each dot represents an individual mouse, and connecting lines indicate samples derived from the same mouse. *$p<0.05$ (one-way ANOVA test with Tukey correction for multiple comparisons). Data represent one representative experiment (n=7 mice) out of two experiments performed. (B) A heatmap showing the normalized expression of genes related to classical T helper polarization: T helper 1 (Th1), T helper 2 (Th2), T helper 17 (Th17), and follicular helper T cells (Tfh), as well as cell-mediated cytotoxicity associated genes. All CD4 T cells were grouped by subset and age (horizontal bars), as in Fig. 2B. (C) T-SNE plots of CD4 T cells colored by normalized expression of cytotoxic-, Th1- and Th17-related genes. (D) Pie charts showing the percentage of cells, within the cytotoxic subset, that were positive either to IFN^+, $IL17a^+$ or both (gating strategy is shown upper left). Each pie chart corresponds to one mouse (n=7).